Long-Term Assessment of the Spatial Temporal Trends in Selected Cloud Physical Properties over the Three Distinct Sites in Kenya

Sostine N. Makokha[1], John W. Makokha[1], Festus B. Kelonye[2]

[1]Department of Science, Technology and Engineering, Kibabii University, Bungoma, Kenya
[2]Department of Biological and Environmental Science, Kibabii University, Bungoma, Kenya
Email: makokhasostine@gmail.com

Abstract

The presence of clouds in the Earth's atmosphere plays a pivotal role in regulating the Earth's energy budget. Increased anthropogenic activities and emissions can significantly lead to changes in cloud composition and cloud structure affecting the clouds physical characteristics, hence causing alterations in the climatic conditions over Kenya. Given this, the present study examined the spatial temporal physical properties of clouds over three study sites, by paying a special consideration on cloud parameters, such as: Cloud Effective Radius (CER), Cloud Top Pressure (CTP), Cloud Top Temperature (CTT) and the Cloud Fraction (CF). These cloud parameters were retrieved from the MODerate resolution Imaging Spectroradiometer (MODIS) sensor and the Modern Era Retrospective analysis for Research and Applications, version 2 (MERRA-2) model between January 2005 and December 2020. The data retrieved on clouds physical properties was utilized to estimate the trends and spatial variations and assess their statistical significance on climate over the study domain. The Spatial patterns of seasonal mean of cloud parameters from the sensors and the model were generally characterized with positive and negative trends over Kenya observed during the four seasons. Trends in CER were found as follows: Nairobi (0.04, 0, −0.04 and −0.01) for the four seasons respectively, Malindi (0.04, 0.01, 0.04 and 0.01) and lastly Mbita (−0.06, −0.06, 0.04 and −0.05); for CTT, Nairobi, −0.1, −0.2, −0.1 and −0.2, Malindi, 0.1, −0.2, 0.1 and 0.05 and Mbita, 0.2, 0.2, −0.2 and 0.15 respectively for every season. Trends in CTP were observed to vary seasonally as follows: Nairobi −0.5, −1, 0.5 and −0.5, Malindi −0.5, −3, 1, and 0.5 and lastly Mbita 0.5, 0, −1 and −1 respectively. And finally, the spatial trends in CF observed over the four seasons over the study domains were obtained a follows: Nairobi (0.3, 0, -0.002 and 0), Malindi (0.3, 0.002, 0 and 0.001) and lastly for Mbita (0.3,

0.003, 0.001 and 0.001) respectively for the four seasons of the study. Spatial trends in the selected cloud properties were determined and observed to vary both seasonally and regionally. The study revealed patterns of trends in physical cloud properties and formed a basis for further research on clouds over Kenya.

Subject Areas

Atmospheric Sciences

Keywords

MODIS, MERRA-2, CF, CER, CTP, CTT Seasons and Clouds Physical Properties

1. Introduction

Clouds form a very crucial component of the atmosphere and play a pivotal role in regulating the Earth's energy budget (Zhang *et al*., 2018) [1]. Apart from other important modulators of climate, Clouds strongly modulate the radiation budget by absorbing and scattering solar and thermal radiation (Roebeling *et al.,* 2006) [2]. In particular, they play a key role in determining the solar radiation reaching the Earth's surface by generally reducing it (by up to nearly 80%) depending mainly on the cloud type, its optical thickness and distribution in the sky (Calbo *et al.,* 2005) [3]. They also interact with the solar radiation causing direct effect such as absorption or scattering (Ichoku *et al.,* 2004) [4].

Cloud center altitude, cloud thickness, crystal number density, condensed matter content, crystal size, cloud top height and cloud fraction are some of the major cloud physical properties of great interest in this research. The interactions of the clouds and other components in the atmosphere cause both predictable and unpredictable weather patterns affecting the climate of the study domain. These simple processes may affect the daily weather patterns over any region and any slightest change in these properties would perturb cloud radiative forcing and modulate the radiative balance of the Earth system (George and Wood, 2010) [5]. Moreover, temporal trends of the changes in intensity, frequency, and duration of temperature and precipitation events are indicators of a changing climate (Audu *et al.,* 2021) [6] caused as a result in variations in cloud characteristics. Clouds physical properties can be assessed through determining the variations in some major cloud parameters such as the Cloud effective radius (CER), Cloud top properties such as the Cloud Top Pressure (CTP), Cloud Top Temperature (CTT) and Cloud Fraction (CF).

Various recent studies have been done on assessing and determining the physical properties of clouds both regionally and globally with the aim of providing knowledge on cloud properties over those study regions. These studies have provided the necessary knowledge on both methods of data acquisition, processing and analysis of the data obtained with an aim of giving it a statistical significance.

Dowling and Radke (1990) [7] examined the physical properties of cirrus clouds in Washington. The study was aimed at examining the cloud center altitude, cloud thickness, crystal number density, and condensed water content and crystal size. The main sources of information and data were from the Lidars (light detection and ranging), Radar systems were also installed in several United States Air Force bases, high quality balloon borne, frost point hygrometers and aircraft measurements. Accurate measurements of the clouds physical properties were not available until these clouds could be reached by properly instrumented aircraft. With limitations of these mentioned techniques, reasonable estimates for typical cirrus crystal concentration, ice water content and crystal length were 30 per liter (range: 10^{-4} to 10^4 per liter), 0.025 gm^{-3} (range: 10^{-4} to 1.2 gm^{-3}) and 250 μm (range: 1 to 8000 μm). The above values were not produced through any formal analysis of the data from the study but instead they represent numbers that were considered consistent with most of the published studies. This research could not form a basis of drawing conclusion on cloud-climate interaction due to lack of consistent data and information.

Further studies were done by Nyasulu *et al.* (2020) [8], this study was carried out on the seasonal climatology and relationship between AOD and cloud properties inferred from the MODIS over Malawi, south east Africa. This study analyzed the spatiotemporal correlations between aerosols and cloud properties during 2008-2017 derived from MODIS over the republic of Malawi. The annual mean AOD at 550 nm (AOD_{550}) was found high (70.23) around the Lake Malawi and its environments and in the southern parts of the study area characterized by dense population and increased anthropogenic activities. The study showed low AOD centers over high altitude locations of central Malawi. The Angstrom Exponent ($AE_{412-470}$) sensitive to fine mode particles was found high (>1.2) in most of the regions during the study period. The trend analysis from the linear regression technique found a general increase in AOD except during the September-October-November season was characterized by decreasing AOD. Relationship between AOD and cloud microphysical properties exhibited a negative correlation with cloud fraction and cloud effective radius. However, it showed a positive correlation with cloud top temperature in areas with high AOD. It was observed that locally derived dust, emissions from industries, vehicles and biomass burning significantly contributed to AOD. These research findings could not point out clearly the effect of variations in aerosol concentrations on climatic variables.

Another study was done by Zhao (Zhao *et al.,* 2019) [9]; a study was carried out in China statistical analysis of cloud characteristics over China using Terra and Aqua MODIS observations on board both NASA Terra and Aqua from March 2003 to February 2018. The study investigated the spatial-temporal variations of both macro and microphysical cloud properties over China; with the cloud parameters CF, CTP, CTT, COT and Effective radius (r_e) of both liquid water and ice clouds (Zhao *et al.,* 2019) [9]. The cloud characteristics were found to vary regionally, seasonally and even depending on the time of the day e.g. morning cloud fraction was found to be different from the afternoon cloud frac-

tion. The variations in the cloud parameters indicated the variation in the weather and the climatic patterns over the study domain providing an insight on what the current study needs to address.

Looking at the above earlier researches and other studies done on physical properties of clouds, it is evident that the clouds micro and macro physical properties vary both seasonally and regionally. Kenya as a country still remains behind in terms of data and knowledge on the physical properties of clouds and the effect of those variations in clouds properties on the Earth's radiation budget. This study seeks to address the knowledge gap over the study sites by assessing the spatial temporal physical properties of clouds over Nairobi, Malindi and Mbita study sites for a period of 16 years from 2005-2020. The cloud parameters assessed by this study were: CF, CER, CTP and CTT (Zhao *et al.,* 2019) [9], Data from MODIS was retrieved for the entire study period and spatial trends and seasonal variations were obtained through a system of algorithms to provide a comprehensive assessment of the clouds physical properties.

2. Materials and Methods

2.1. Study Area

The study was conducted over Kenya, a region that is bounded by Latitudes 5˚S - 5˚N and Longitudes, 34˚E - 42˚E. Kenya is an East African country bordered by Ethiopia to the North, Tanzania to the South, South Sudan to the North-west, Uganda to the West and lastly Somalia to the East. The proposed study was done over the Republic of Kenya over three main environmentally distinct regions. The regions of focus were: Nairobi (1˚S, 36˚E), Mbita (0˚S, 34˚E) and Malindi (4˚S, 40˚E) (Figure 1).

Nairobi is 1669 m high above the sea level (Mideva, E. M. 2021) [10]. The
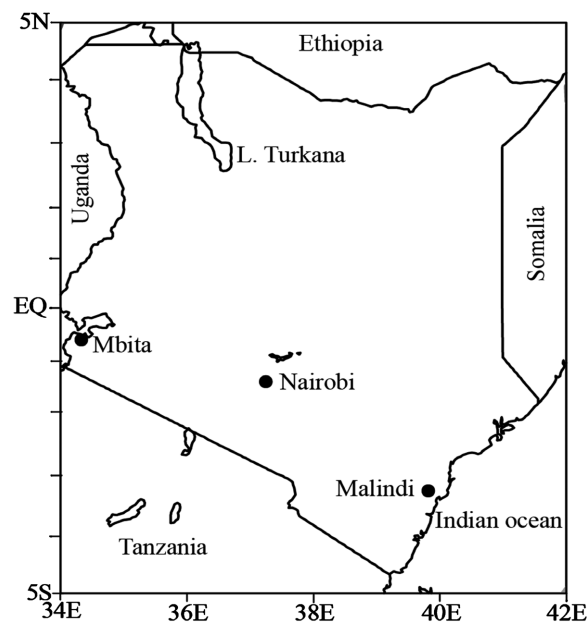

Figure 1. Map of Kenya showing the three study sites in Kenya.

Nairobi region represents the urban climate. The main contributors to the cloud content and characteristics are anthropogenic as a result of industrial-vehicular emissions (Makokha *et al.,* 2013) [11] in the Nairobi area. The climate here is warm and temperate, and a significant amount of rainfall is received throughout including in the driest month of the year. The annual rainfall is 674mm while the average temperature is 18.8˚C. Nairobi has the highest population about 4.397 million people according to the Kenya National Bureau of Statistics (KNBS, 2019) [12].

Malindi is a town in Kilifi County on Malindi bay at the mouth of Sabaki River lying on the Indian Ocean coast of Kenya. It is 120 km north-east of Mombasa with a population of 119,859 (KNBS Census 2019) [12] with an elevation of 118 m above the sea level. According to Koppen-Geiger climate classification of climate, Malindi has a hot tropical type of climate with a winter dry season with an average temperature of about 26.2˚C. Malindi receives much rain during summer than winter according to the Kopper-Geiger and an annual rainfall of 755 mm. Malindi borders the Indian Ocean and as a result, it experiences the maritime atmosphere which is its largest contributors of the cloud content and properties.

Mbita region is in Homabay county on the shores of Lake Victoria, 1125 m above the sea level (Boiyo *et al.,* 2018) [13], with a population of approximately 14,916 (KNBS, 2019) [12]. Mbita in this present study represents the Kenyan rural atmosphere. Mbita experiences tropical type of climate and receives an average annual rainfall of approximately 1259.3 mm (Bakayoko *et al.,* 2021) [14] even the driest month still has a lot of rainfall. The annual average temperatures for Mbita are about 23.7˚C.

Based on the prevailing meteorological conditions, a year was then divided into four seasons. December-January-February (DJF), March-April-May (MAM), June-July-August (JJA) and lastly, the September-October-November (SON) seasons. The DJF and JJA represents the local dry seasons characterized by reduced rainfall (Khamala *et al.*, 2022) [15] while the MAM and SON seasons representing the local wet seasons characterized by enhanced rainfall (Khamala *et al.*, 2022 [15]; Boiyo *et al.*, 2018 [16]).

2.2. MODIS Satellite Sensor

MODerate Imaging Spectroradiometer (MODIS) is a Polar-orbiting satellite sensor launched into the Earth orbit by National Aeronautics and Space Administration (NASA) (Barnes *et al.,* 2003) [17] Goddard Space Flight Center on board the Terra (morning orbit) on 18th December 1999 and Aqua (afternoon orbit) satellite launched on 4th May 2002 (Khamala *et al.*, 2022 [15]; Mito *et al.*, 2012 [18]; Remer *et al.*, 2005 [19]). With a band of ~2330 km and time-based (Temporal) resolution of 1 - 2 days (King *et al.,* 2013) [20], and acquires data globally over 36 spectral bands ranging in wavelengths from 0.415 to 14.235 μm at three spatial resolutions (2 bands at 250 m, 5 bands at 500 m, and 29 bands at 1 km). MODIS is a 36-band Spectroradiometer that provides several cloud proper-

ties using the spectral bands from visible to thermal infrared (Cao *et al.,* 2013) [21].

MOD08-D3 product is also used, which includes daily measurements of optical thickness, cloud top pressure and effective particle radius (Platnick *et al.,* 2003) [22] gridded at a latitude and longitude resolution of 1˚ × 1˚ (roughly 100 km × 100 km at mid-latitudes). The clouds and Earth's Radiant energy system (CERES) is also a radiometer also on board the Terra and Aqua platforms. CERES measures the radiation on top of the atmosphere in three channels; the first channel is a shortwave channel for the solar reflected radiation in 0.3 - 5 μm, the second channel measures the Earth's surface emitted radiation in the atmospheric window of 8 - 12 μm and lastly, the third channel measures the whole spectrum. MODIS datasets are very important for collecting various statistics on cloud microphysical properties as a result of aerosols (Platnick *et al.,* 2016) [23]. For water vapor, the retrieval for the near infrared region is used. MODIS uses an infrared band to determine the physical properties of clouds in relation to CTT and CTP. Visible and near infrared bands are used to determine the optical and microphysical cloud properties. (Alam *et al.,* 2010) [24].

Daily global level 2 data are provided whereby the cloud particle, phase effective cloud, particle radius and cloud optical thickness are derived using the near infrared channel radiances. Also, the cloud top height, effective emissivity, phases and cloud fraction are produced by the infrared retrieval methods day and night at 5 × 5 1-km pixel resolution. In summary, MODIS measures the cloud top properties (temperature, pressure and effective emissivity), cloud thermodynamic phase and cloud optical and microphysical parameters (optical thickness, effective particle radius and water path). The MODIS resolution ranges between 0.25 to 1 km (Platnick *et al.,* 2003) [22].

The present study utilized the level 3 monthly data on cloud parameters retrieved from MODIS Terra at a spatial resolution of 1˚ × 1˚ for a period of 16 years (January 2005 to December 2020) to study trends and their significance levels over Kenya. These data products were sourced from http://giovanni.gsfc.nasa.gov/giovanni/. The MODIS datasets are preferred because they are open to the public and more precise to spatial and temporal distribution. The dataset can also enable one to find an empirical relationship between the reflectivity and the microphysical cloud properties which in turn can derive a conclusion of variations of cloud physical properties on climatic variables.

2.3. MERRA-2 Model

The Modern-Era Retrospective Analysis and Research and Application, version 2 (MERRA-2) atmospheric reanalysis product was newly released and launched by NASA Global Modeling and Assimilation Office (GMAO) to provide data since 1980 (Randles *et al.,* 2017) [25]. MERRA-2 replaced the original MERRA dataset (Bosilovich *et al.,* 2015) [26] because of the advances made in the assimi-

lation system that enable assimilation of modern hyper spectral radiances and microwave observations. Also uses NASA's Ozone profile observations that began in the late 2004. The model is based on the version of the GEOS-5 atmospheric data from 1980 to 2016 at $0.5° \times 0.625°$ resolution with 72 layers and spanning the satellite observing era from 1980 to the present (Khamala *et al.,* 2022) [15].

Along with the enhancements in the meteorological assimilation, MERRA-2 takes some significant steps towards GMAO's targets of an earth system reanalysis. In the present study, MERRA-2 M2TMNXAER v5.12.4 level-3 monthly time-averaged data on cloud parameters were retrieved at a spatial resolution of $0.5° \times 0.625°$ from January 2005 to December 2020. These data products were sourced from http://giovanni.gsfc.nasa.gov/giovanni/.

2.4. Methods

This section highlights the suitable methods used during the analysis of the data retrieved from MODIS and MERRA-2 in order to obtain any significant statistical interpretation of the data obtained.

2.4.1. Linear Regression Analysis

Determination of the combined effect of cloud physical and radiative properties on the climatic parameters such as precipitation rate makes use of the linear regression analysis. Linear regression provides very crucial information and direction on how well a set of variables can predict a particular outcome. It focuses on the conditional probability distribution of the response given the values of the predictors, rather than on the joint probability distribution of all of these variables. The Linear Regression makes use of the following derivation; let Y denote the "dependent" variable whose values you wish to predict and let $X_1, \cdots, X_k$ denote the "independent" variable from which you wish to predict it, with the value of variable X in the period t (or in row t of the dataset) denoted by X_{1t}. Then the equation for computing the predicted value of Y_t is given by;

$$Y_t = b_0 + b_1 X_{1t} + b_2 X_{2t} + \cdots + b_k X_k \tag{1}$$

where Y is a straight-line function of each of the X-variable holding others constant, the contributions of different X variables to the predictions are additive.

$b_1, b_2, \cdots, b_k$ are the slopes of their individual straight-line relationships with Y, the coefficients of the variables, b_0, the intercept is the prediction that the model would make if the $X's$ were zero. The coefficients and intercept are estimated by least squares *i.e.*, setting them equal to the unique values that minimize the sum of squared errors within the sample of data to which the model is fitted. And the model's prediction errors are typically assumed to be independently and identically normally distributed.

2.4.2. Trend Analysis

The study has determined the spatial and temporal variation of clouds physical properties through assessing the variations in cloud parameters using trend analysis to determine the variability of the trends in Kenya. Numerous statistical

methods exist to quantify trends in the time series of a geophysical variable, Mann Kendall test has been used by this present study to evaluate annual, seasonal and monthly trends of climatic variables (Audu *et al.*, 2021) [6] such as CTP and CTT for the selected regions in Kenya over a 16-year period (2005-2020) (Syed *et al.*, 2021) [27]. The test has been found to be the most appropriate for analysis of climatic changes in climatological time series for detection of a climatic discontinuity (Wanjuhi, 2016) [28].

The method is applied to the long-term data in this study to detect statistically significant trends and the method is preferred when various stations are tested in a single study (Mondal *et al.*, 2012) [29], and for this study, Nairobi, Malindi and Mbita clouds can be studied at the same time using this Mann Kendall test. In this test the null hypothesis (H$_o$) is that there has been no trend in precipitation over time the alternative hypothesis (H$_1$) is that there has been a trend (increasing or decreasing) over time.

The mathematical equations for calculating Mann-Kendall statistics *S*, *V*(*s*) and standardized test statistics *Z* are as follows:

$$S = \sum_{i=l}^{n-l} \sum_{j=i+1}^{n} sig\left(X_j - X_i\right) \tag{2}$$

The application of trend test is done to a time series X_i that is ranked $i = 1, 2, \cdots, n-1$ and X_j, which is ranked from $j = i+1, 2, \cdots, n$ (Mondal *et al.*, 2012) [29]; Yadav *et al.*, 2014 [30]). Each of the data products X_i is taken as the reference point which is compared with the rest of the data points X_j so that:

$$Sgn\left(X_j - X_i\right) = \left\{H\ H\left(x_j - x_i\right)\right\} = 0 \tag{3}$$

$$Sgn\left(X_j - X_i\right) = \begin{cases} +1 & \text{if } \left(X_j - X_i\right) > 0 \\ 0 & \text{if } \left(X_j - X_i\right) = 0 \\ -1 & \text{if } \left(X_j - X_i\right) < 0 \end{cases} \tag{3}$$

$$V(s) = \frac{1}{18} n(n-1)(2n+5) - \sum_{p=1}^{q} t_p \tag{4}$$

Equations (3) and (4) yields a standard normal distribution factor *Z* given by:

$$Z = \begin{cases} \dfrac{s-1}{\sqrt{VAR(s)}} & \text{if } s > 0 \\ 0 & \text{if } s = 0 \\ \dfrac{s+1}{\sqrt{VAR(s)}} & \text{if } s < 0 \end{cases} \tag{5}$$

A positive value of *Z* *i.e.* ($Sgn\left(X_j - X_i\right)$) signifies an upward trend while a negative value of *Z* signifies a downward trend in the time series observations in chronological order (Mondal *et al.*, 2012) [29].

In these equations,

X_i and X_j = are the time series observations in chronological order

n is the length of time series

t_p is the number of ties for p^{th} value

q is the number of tied values

Positive Z-values indicate an upward trend in the hydrologic time series.

Negative Z-values indicate a negative trend. If $|Z| > Z_{1-\alpha/2}$, (H$_0$) is rejected and a statistically significant trend exist in the hydrologic time series.

The critical value of $Z_{1-\alpha/2}$ for a p value of 0.05 from the standardized normal table is 1.96 (Ahmad *et al.*, 2015) [31]. In the present work, linear regression analysis was used to estimate monthly trends in key cloud parameters (CTP, CTT and CER). The method has been discussed widely by Weatherhead *et al.*, (1998) [32]. This test also assists in determining the variations of the climatic variables with time for the period between the year 2005 and 2020.

3. Results and Discussions

3.1. Trends in Cloud Effective Radius

Cloud effective radius (CER) refers to the weighted mean of the size distribution of cloud droplets. Cloud Effective Radius can also be defined as the ratio of the third to the second moment of droplet size distribution. The trends in Cloud effective radius retrieved from MODIS data were observed to vary both seasonally and spatially ranging from positive to negative trends as obtained during the whole study period (Figure 2).

Positive seasonal trends in CER are observed in all seasons for the Malindi clouds. Positive trends in DJF season over Nairobi with negative trends in both JJA and SON seasons over Nairobi clouds. And lastly negative trends over Mbita clouds except during the JJA season. It is observed that cloud over Malindi has the highest average CER in all the four seasons as compared to Nairobi and Mbita clouds over the whole study period. CER is higher over oceans than over the ground (King *et al.*, 2013) [20]. Furthermore, it is noted that the effective radius of the polluted cloud will decrease when compared to the pristine cloud (Saponaro, G. 2020) [33] and for this reason, clouds over Nairobi region have the smallest effective radius due to the net industrial emissions of gases and other pollutants from the industries, biomass burning and vehicular emissions.

3.2. Trends in Cloud Top Pressure

Cloud top pressure is another key cloud parameter measured in hectopascals that can greatly provide in-depth understanding of cloud characteristics and the climate. The trends in CTP obtained during the study period were obtained and the spatial variation maps depicting the CTP over Kenya also drawn in order to obtain the general trends and significance of the trends on the climate of the study domains as shown in Figure 3.

The trends in CTP vary with seasons stated and this provides the sufficient knowledge on how cloud top pressure varies over the study regions as expected by the objectives of this study. Negative trends in CTP over Nairobi and Malindi during the DJF and MAM seasons were observed and positive trends over Mbita
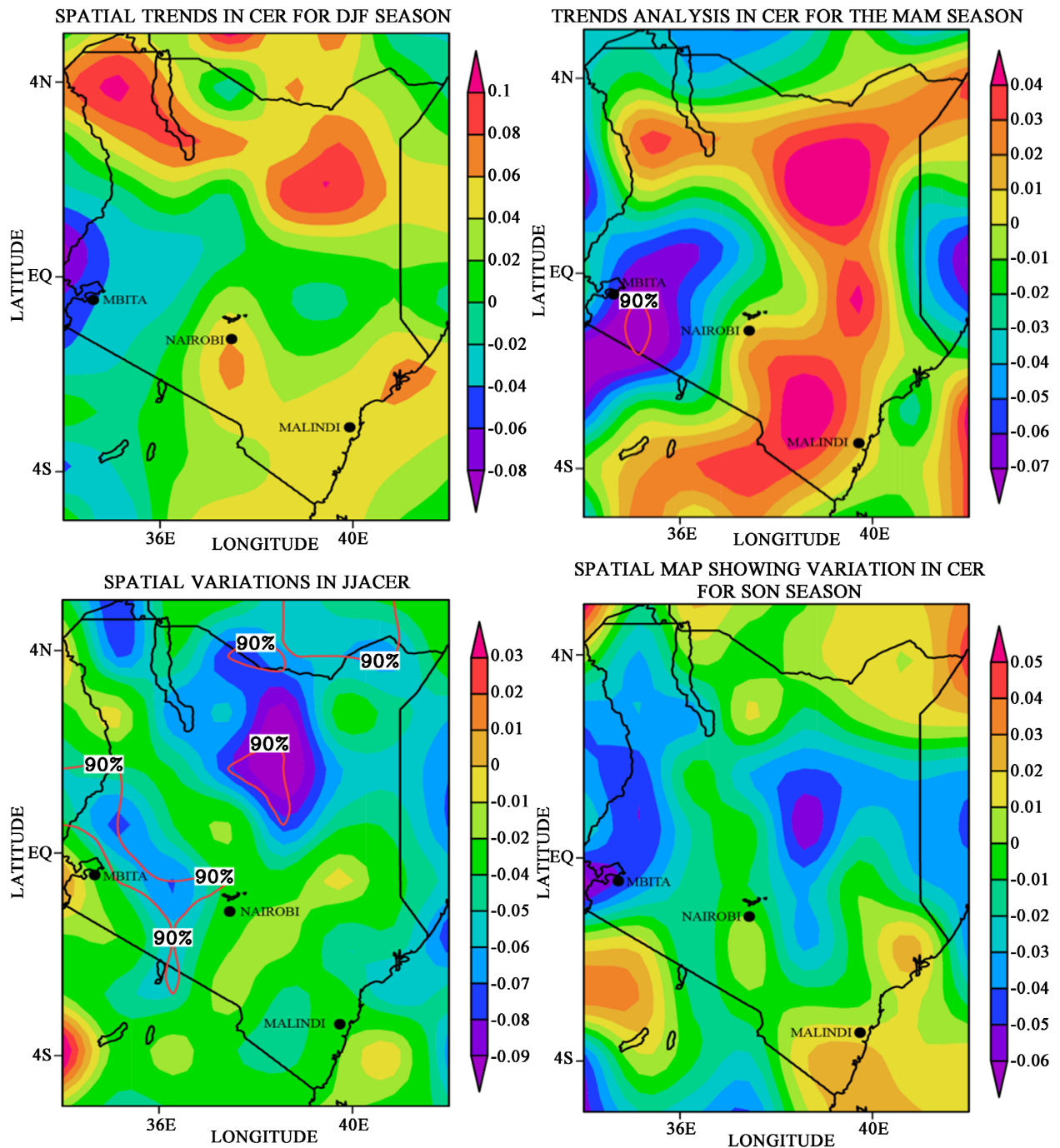
Figure 2. Spatial maps of Kenya showing trends in CER for the four seasons.

during the DJF season and no significant trend in MAM season over Mbita were also observed. Negative trends in CTP over Mbita during the JJA season and positive trends over Nairobi and Malindi during the JJA season. And lastly, Malindi had positive trends while Nairobi and Mbita having negative trends in CTP during the SON season.

The higher the CTP the cooler, the particles and hence lower emission rate. It is therefore clear that clouds over Malindi are cooler with lowest emission rate
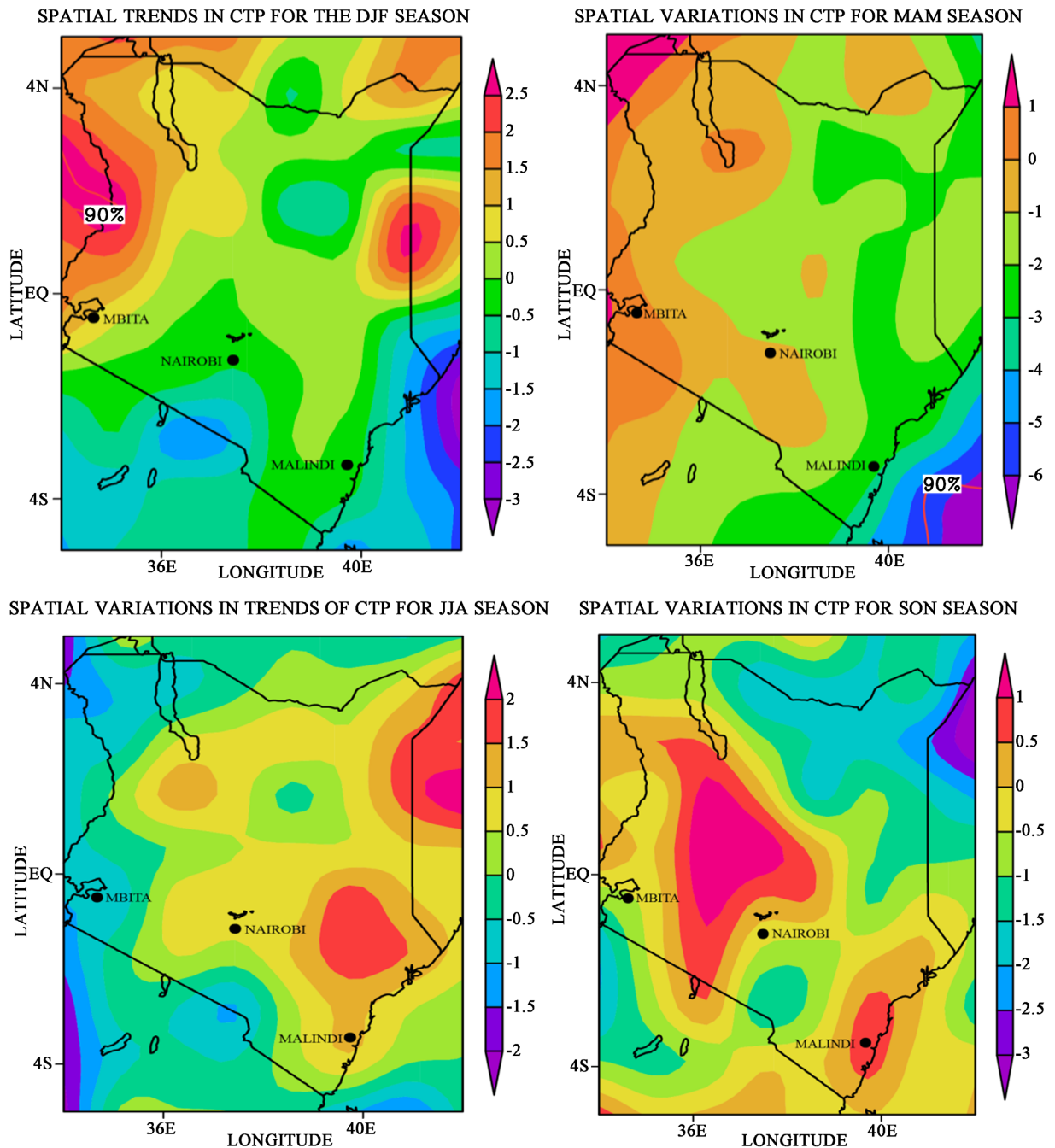
Figure 3. Spatial maps of Kenya showing trends in CTP for the four seasons.

followed by those over Mbita and lastly over Nairobi having warmer particles with the highest emission rate.

3.3. Trends in Cloud Top Temperature

Cloud top temperature refers to the atmospheric temperature at the level of the cloud top. Cloud top temperature plays an important role in the net earth radiation budget studies (Liu *et al.,* 2020) [34]. The product can be used to monitor cloud-top changes during convection (Lensky, I.M. and Rosenfeld, D. 2006)

[35]. Nairobi posted negative trends in CTT in seasonal trends for all the four seasons. Positive seasonal trends for Malindi except during the MAM season and lastly, positive during the DJF and MAM seasons for CTT over Mbita clouds. Aerosols normally act on the clouds so as to change cloud particle size near the cloud top (Williams, A.S. and Igel. A.L. 2021) [36], optical thickness and fraction but to keep the cloud top temperature without causing a significant long wave radiative forcing (**Figure 4**).
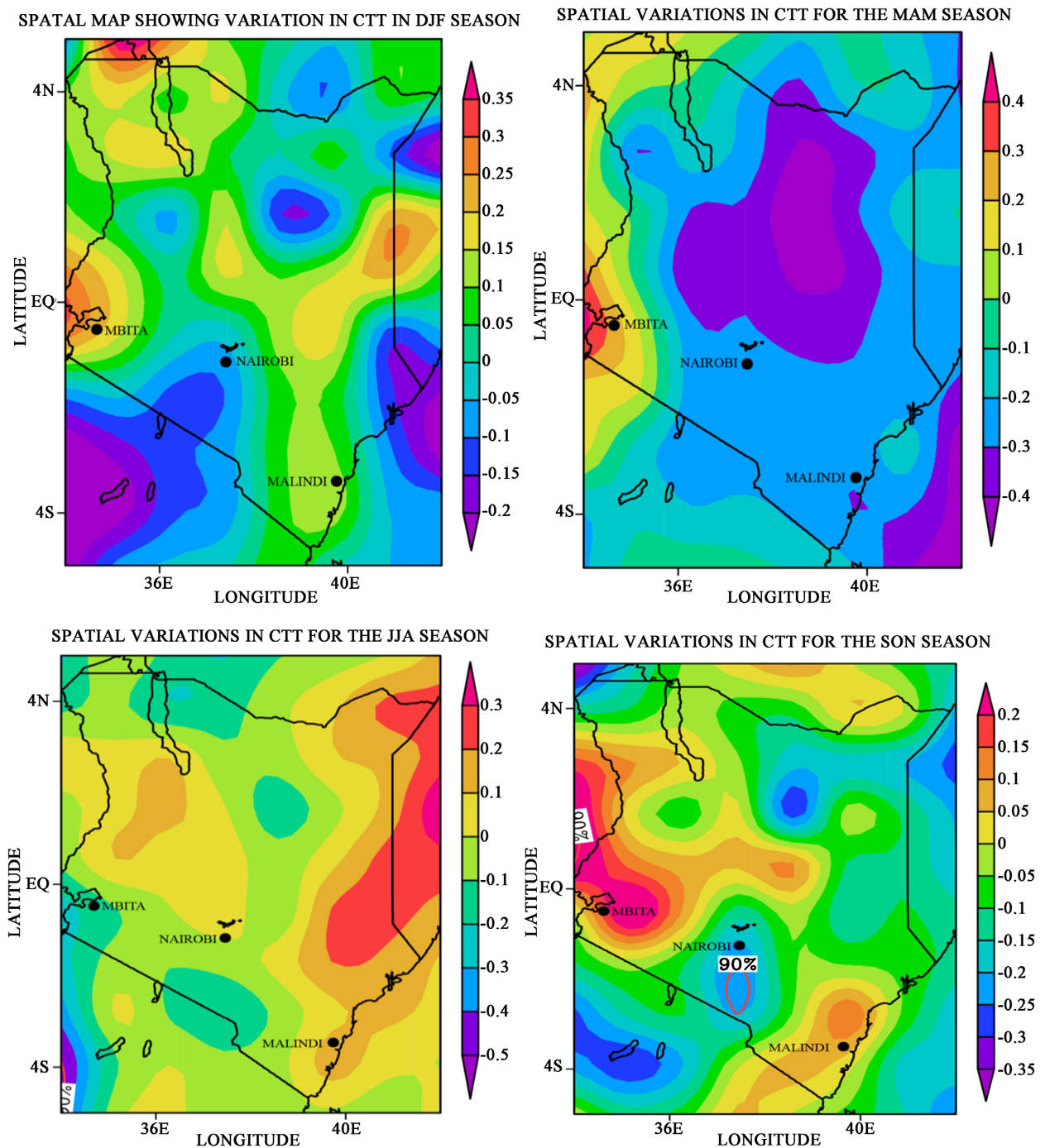

Figure 4. Spatial maps of Kenya showing the trends in CTT in the four seasons.
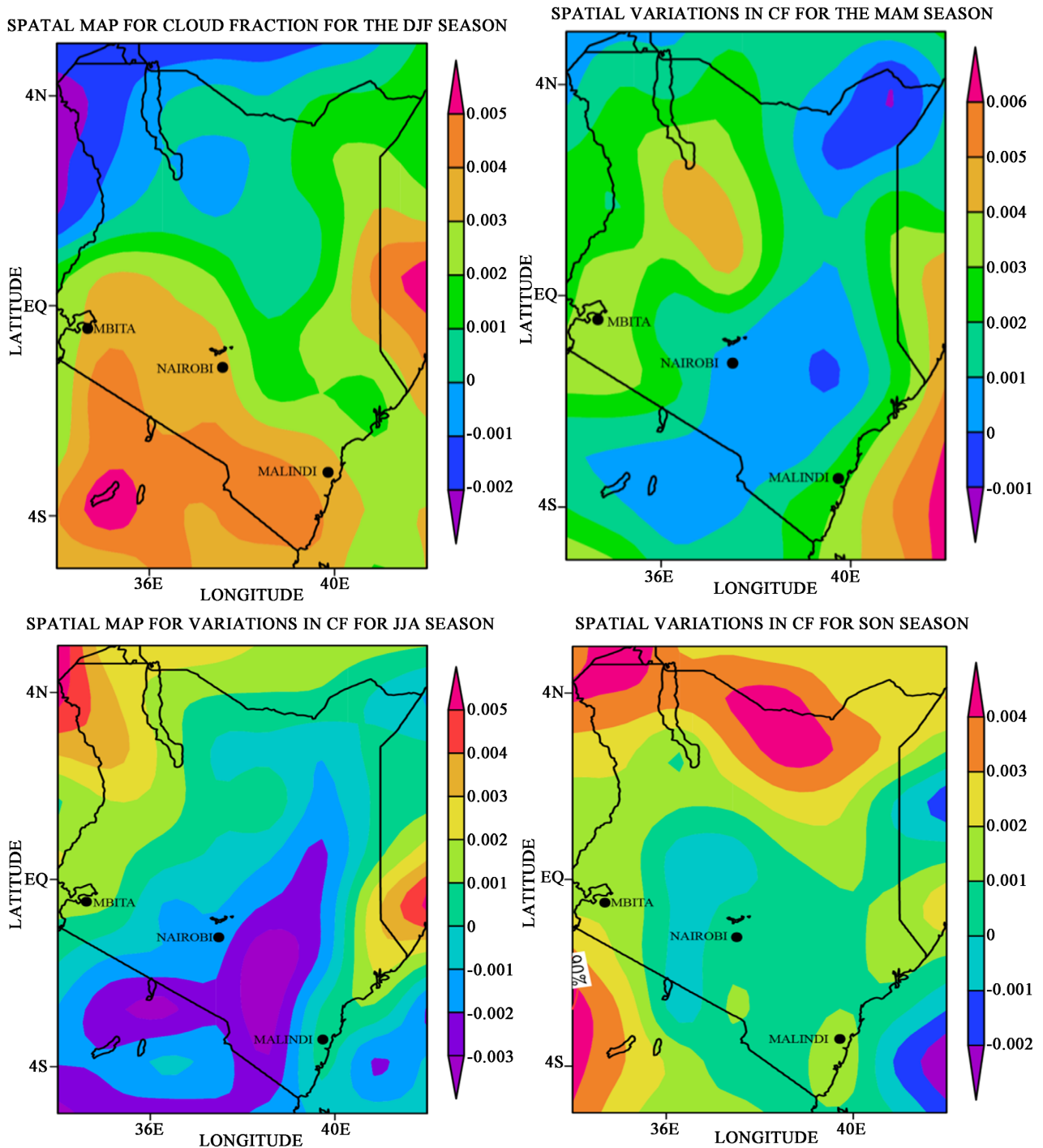
Figure 5. Spatial maps of Kenya showing trends in CF for the four seasons.

3.4. Trends in Cloud Fraction

Cloud fraction refers to the fraction of the sky obscured by the clouds when observed from a particular location (http://www.cloudfraction). Cloud fraction is also a very crucial aspect to consider when investigating clouds physical properties. CF is measured in Oktas ranging from the values 0 to 4 where 0 Oktas represents absence of clouds while 4 Oktas representing total cloud cover (TCC)

(Pliemon *et al.*, 2022) [37]. It is observed that the fraction of clouds varies from one region to another depending on some factors such as the natural evaporation of the water bodies and the anthropogenic human activities such as burning of surface wastes and land surfaces during preparation stages for agricultural activities. Figure 5 represents the values obtained for CF during the study period from MODIS terra and employment of a series of arithmetics which provided the spatial maps showing the variation in cloud fraction.

4. Summary and Conclusions

Using the data sets retrieved from MODIS sensor and MERRA-2 model, the present study revealed an in depth understanding of trends in CER, CTT, CTP and CF as well as the spatial distribution in the above parameters over Kenya for the period 2005-2020 (Table 1). The spatial variations in cloud parameters from MODIS-sensor and the MERRA-2 model were used to infer on the general physical properties of clouds over the three study sites.

The study domains were dominated by positive trends in most of the cloud parameters, with a significance of 90% in most of the seasons. The variation in trends in clouds physical properties is attributed to biomass burning, vehicular and industrial emissions that contributes to foreign materials into the atmosphere over the study domain.

The study domain was dominated by negative trends in CER, CTP and CTT

Table 1. Spatial trends in cloud parameters over the study sites (January 2005-December 2020).

Cloud property	Season	Nairobi	Malindi	Mbita
Cloud fraction	DJF	0.3	0.3	0.3
	MAM	0	0.002	0.003
	JJA	−0.002	0	0.001
	SON	0	0.001	0.001
Cloud effective radius	DJF	0.04	0.04	−0.06
	MAM	0	0.01	−0.06
	JJA	−0.04	0.04	0.04
	SON	−0.01	0.01	−0.05
Cloud top pressure	DJF	−0.5	−0.5	0.5
	MAM	−1	−3	0
	JJA	0.5	1	−1
	SON	−0.5	0.5	−1
Cloud top temperature	DJF	−0.1	0.1	0.2
	MAM	−0.2	−0.2	0.2
	JJA	−0.1	0.1	−0.2
	SON	−0.2	0.05	−0.15

except for CER over Malindi in all seasons and Nairobi during the DJF and MAM seasons. Seasonally, positive trends in cloud fraction (CF) were observed in all the season over the study domain due to changes in climatic condition and anthropogenic activities such as biomass burning and both vehicular and industrial emissions which increases the cloud lifetime and aerosols acting as the condensation nuclei in the atmosphere increasing the cloud formation.

The study domain significantly exhibited decreasing and increasing trends in all the cloud parameters over the study period clearly indicating variations in clouds physical properties caused as a result of different clouds contributors and modulators of cloud characteristics.

The knowledge on spatial trends and spatial distribution maps is very important. Both seasonal and regional variations in clouds parameters would mean variations in climatic variables which then form a basis of understanding the concepts of climatic variations and climate change. This important information and data is lacking over Kenya, hence opening a link and a need for further investigation and research on clouds physical properties.

Acknowledgements

Conflicts of Interest

The authors declare no conflicts of interest.

References

[1] Zhang, J., Liu, P., Zhang, F. and Song, Q. (2018) Cloud Net: Ground-Based Cloud Classification with Deep Convolutional Neural Network. *Geophysical Research Letters*, **45**, 8665-8672. https://doi.org/10.1029/2018GL077787

[2] Roebeling, R.A., Feijt, A.J. and Stammes, P. (2006) Cloud Property Retrievals for Climate Monitoring: Implications of Differences between Spinning Enhanced Visible and Infrared Imager (SEVIRI) on METEOSAT-8 and Advanced Very High Resolution Radiometer (AVHRR) on NOAA-17. *Journal of Geophysical Research*: *Atmospheres*, **111**, 1-16. https://doi.org/10.1029/2005JD006990

[3] Calbo, J., Pages, D. and Gonzale, J. (2005) Empirical Studies of Cloud Effects on UV Radiation: A Review. *Review Geophysics*, **43**, 1-28. https://doi.org/10.1029/2004RG000155

[4] Ichoku C., Kaufman, Y.J., Remor, L.A. and Levy, R. (2004) Global Aerosol Remote Sensing from MODIS. *Advances in Space Research*, **34**, 820-827. https://doi.org/10.1016/j.asr.2003.07.071

[5] George, R.C. and Wood, R. (2010) Subseasonal Variability of Low Cloud Radiative Properties over the Southeast Pacific Ocean. *Atmospheric Chemistry and Physics*,

10, 4047-4063. https://doi.org/10.5194/acp-10-4047-2010

[6] Audu, M.O., Ejembi, E. and Igbawua, T. (2021) Assessment of Spatial Distribution and Temporal Trends of Precipitation and Its Extremes over Nigeria. *American Journal of Climate Change*, **10**, 331-352. https://doi.org/10.4236/ajcc.2021.103016

[7] Dowling, D.R. and Radke, L.F. (1990) A Summary of the Physical Properties of Cirrus Clouds. *Journal of Applied Meteorology and Climatology*, **29**, 970-978. https://doi.org/10.1175/1520-0450(1990)029<0970:ASOTPP>2.0.CO;2

[8] Nyasulu, M., Haque, M.M., Boiyo, R., Kumar, K.R. and Zhang, Y.L. (2020) Seasonal Climatology and Relationship between AOD and Cloud Properties Inferred from the MODIS over Malawi, Southeast Africa. *Atmospheric Pollution Research*, **11**, 1933-1952. https://doi.org/10.1016/j.apr.2020.07.023

[9] Zhao, C.F., Chen, Y.Y., Li, J.M., Letu, H., Su, Y.F., Chen, T.M. and Wu, X.L. (2019) Fifteen-Year Statistical Analysis of Cloud Characteristics over China Using Terra and Aqua Moderate Resolution Imaging Spectroradiometer Observations. *International Journal of Climatology*, **39**, 2612-2629. https://doi.org/10.1002/joc.5975

[10] Mideva, E.M. (2021) Atrium Daylight Penetration in Dense Apartment Blocks. A Case of Roysambu Nairobi, Kenya. University of Nairobi School of the Environment Department of Architecture and Building Science, Nairobi.

[11] Makokha, J.W., Kimani, J.N. and Angeyo, H.K. (2013) Estimation of Radiative Forcing Due to Aerosols over Selected Sites in Kenya. *Journal of meteorological Research*, **6**, 3-13.

[12] KNBS and Republic of Kenya (2019) 2019 Kenya Population and Housing Census: Vol. 1: Population by County and Sub-County.

[13] Boiyo, R.K., Kumar, R. and Zhao, T. (2018) Optical, Microphysical and Radiative Properties of Aerosols over a Tropical Rural Site in Kenya, East Africa: Source Identification, Modification and Aerosols Type Discrimination. *Journal Atmospheric Environment*, **177**, 234-252. https://doi.org/10.1016/j.atmosenv.2018.01.018

[14] Bakayoko, A., Galy-Lacaux, C., Yoboué, V., Hickman, J.E., Roux, F., Gardrat, E. and Delon, C. (2021) Dominant Contribution of Nitrogen Compounds in Precipitation Chemistry in the Lake Victoria Catchment (East Africa). *Environmental Research Letters*, **16**, Article ID: 045013. https://doi.org/10.1088/1748-9326/abe25c

[15] Khamala, G.W., Makokha, J.W., Boiyo, R. and Kumar, K.R. (2022) Long-Term Climatology and Spatial Trends of Absorption, Scattering, and Total Aerosol Optical Depths over East Africa during 2001-2019. *Environmental Science and Pollution Research*, **29**, 61283-61297. https://doi.org/10.1007/s11356-022-20022-6

[16] Boiyo, R., Kumar, K.R., Zhao, T. and Bao, Y. (2017) Climatological Analysis of Aerosol Optical Properties over East Africa Observed from Space-Borne Sensors during 2001-2015. *Atmospheric Environment*, **152**, 298-313. https://doi.org/10.1016/j.atmosenv.2016.12.050

[17] Barnes, W.L., Xiong, X., Guenther, B.W. and Salomonson, V. (2003) Development, Characterization, and Performance of the EOS MODIS Sensors. *Earth Observing Systems VIII*, **5151**, 337-345. https://doi.org/10.1117/12.504818

[18] Mito, C.O., Boiyo, R.K. and Laneve, G. (2012) A Simple Algorithm to Estimate Sensible Heat flux from Remotely Sensed MODIS Data. *International Journal of Remote Sensing*, **33**, 6109-6121. https://doi.org/10.1080/01431161.2012.680616

[19] Remer, L.A., Kaufman, Y.J., Tanré, D., Mattoo, S., Chu, D.A., Martins, J.V. and Holben, B.N. (2005) The MODIS Aerosol Algorithm, Products, and Validation. *Journal of the Atmospheric Sciences*, **62**, 947-973. https://doi.org/10.1175/JAS3385.1

[20] King, M.D., Platnick, S., Menzel, W.P., Ackerman, S.A. and Hubanks, P.A. (2013) Spatial and Temporal Distribution of Clouds Observed by MODIS Onboard the Terra and Aqua Satellites. *IEEE Transactions on Geoscience and Remote Sensing*, **51**, 3826-3852. https://doi.org/10.1109/TGRS.2012.2227333

[21] Cao, C., De Luccia, F.J., Xiong, X., Wolfe, R. and Weng, F. (2013) Early On-Orbit Performance of the Visible Infrared Imaging Radiometer Suite Onboard the Suomi National Polar-Orbiting Partnership (S-NPP) Satellite. *IEEE Transactions on Geoscience and Remote Sensing*, **52**, 1142-1156. https://doi.org/10.1109/TGRS.2013.2247768

[22] Platnick, S., King, M., Ackerman, S., Menzel, W., Baum, B., Riedi, J. and Frey, R. (2003) The MODIS Cloud Products: Algorithms and Examples from Terra. *IEEE Transactions on Geoscience and Remote Sensing*, **41**, 459-473. https://doi.org/10.1109/TGRS.2002.808301

[23] Platnick, S., Meyer, K.G., King, M.D., Wind, G., Amarasinghe, N., Marchant, B., Riedi, J., *et al.* (2016) The MODIS Cloud Optical and Microphysical Products: Collection 6 Updates and Examples from Terra and Aqua. *IEEE Transactions on Geoscience and Remote Sensing*, **55**, 502-525. https://doi.org/10.1109/TGRS.2016.2610522

[24] Alam, K., Iqbal, M.J., Blaschke, T., Qureshi, S. and Khan, G. (2010) Monitoring Spatio-Temporal Variations in Aerosols and Aerosol-Cloud Interactions over Pakistan Using MODIS Data. *Advances in Space Research*, **46**, 1162-1176. https://doi.org/10.1016/j.asr.2010.06.025

[25] Randles, C.A., Da Silva, A.M., Buchard, V., Colarco, P.R., Darmenov, A., Govindaraju, R. and Flynn, C.J. (2017) The MERRA-2 Aerosol Reanalysis, 1980 Onward. Part I: System Description and Data Assimilation Evaluation. *Journal of climate*, **30**, 6823-6850. https://doi.org/10.1175/JCLI-D-16-0609.1

[26] Bosilovich, M.G., Lucchesi, R. and Suarez, M. (2015) MERRA-2: File Specification. Global Modeling and Assimilation Office, Maryland.

[27] Syed, A., Liu, X.P., Moniruzzaman, M., Rousta, I., Syed, W., Zhang, J. and Olafsson, H. (2021) Assessment of Climate Variability among Seasonal Trends Using *in Situ* Measurements: A Case Study of Punjab, Pakistan. *Atmosphere*, **12**, Article 939. https://doi.org/10.3390/atmos12080939

[28] Wanjuhi, D.M. (2016) Assessment of Meteorological Drought Characteristics in North Eastern Counties of Kenya. Doctoral Dissertation, University of Nairobi, Nairobi.

[29] Mondal, A., Kundu, S. and Mukhopadhyay, A. (2012) Rainfall Trend Analysis by Mann-Kendall Test: A Case study of North-Eastern Part of Cuttack District, Orissa. *International Journal of Geology, Earth and Environmental Sciences*, **2**, 70-78.

[30] Yadav, R., Tripathi, S.K., Pranuthi, G. and Dubey, S.K. (2014) Trend Analysis by Mann-Kendall Test for Precipitation and Temperature for Thirteen Districts of Uttarakhand. *Journal of Agrometeorology*, **16**, 164-171. https://doi.org/10.54386/jam.v16i2.1507

[31] Ahmad, I., Tang, D., Wang, T., Wang, M. and Wagan, B. (2015) Precipitation Trends over Time Using Mann-Kendall and Spearman's rho Tests in Swat River Basin, Pakistan. *Advances in Meteorology*, **2015**, Article ID: 431860. https://doi.org/10.1155/2015/431860

[32] Weatherhead, E.C., Reinsel, G.C., Tiao, G.C., Meng, X.L., Choi, D., Cheang, W.K. and Frederick, J.E. (1998) Factors Affecting the Detection of Trends: Statistical Considerations and Applications to Environmental Data. *Journal of Geophysical*

Research: *Atmospheres*, **103**, 17149-17161. https://doi.org/10.1029/98JD00995

[33] Saponaro, G. (2020) Application of Remotely-Sensed Cloud Properties for Climate Studies. *Journal of Geophysical Research*: *Atmospheres*, **185**, 1-5. http://hdl.handle.net/10138/308930

[34] Liu, C.Y., Chiu, C.H., Lin, P.H. and Min, M. (2020) Comparison of Cloud-Top Property Retrievals from Advanced Himawari Imager, MODIS, CloudSat/CPR, CALIPSO/CALIOP, and Radiosonde. *Journal of Geophysical Research*: *Atmospheres*, **125**, 1-11. https://doi.org/10.1029/2020JD032683

[35] Lensky, I.M. and Rosenfeld, D. (2006) The Time-Space Exchangeability of Satellite Retrieved Relations between Cloud Top Temperature and Particle Effective Radius. *Atmospheric Chemistry and Physics*, **6**, 2887-2894. https://doi.org/10.5194/acp-6-2887-2006

[36] Williams, A.S. and Igel, A.L. (2021) Cloud Top Radiative Cooling Rate Drives Non-Precipitating Stratiform Cloud Responses to Aerosol Concentration. *Geophysical Research Letters*, **48**, 1-11. https://doi.org/10.1029/2021GL094740

[37] Pliemon, T., Foelsche, U., Rohr, C. and Pfister, C. (2022) Subdaily Meteorological Measurements of Temperature, Direction of the Movement of the Clouds, and Cloud Cover in the Late Maunder Minimum by Louis Morin in Paris. *Climate of the Past Discussions*, **18**, 1-39. https://doi.org/10.5194/cp-2021-179